ELSEVIER

Thermochimica Acta 268 (1995) 121–142

thermochimica acta

# Modulated differential scanning calorimetry: isothermal cure and vitrification of thermosetting systems

G. Van Assche, A. Van Hemelrijck, H. Rahier, B. Van Mele*

*Department of Physical Chemistry and Polymer Science, Vrije Universiteit Brussel, Pleinlaan 2, 1050 Brussels, Belgium*

Received 18 July 1995; accepted 1 August 1995

**Abstract**

Modulated differential scanning calorimetry (MDSC) is used to study simultaneously the evolution of heat flow and heat capacity for the isothermal cure of thermosetting systems. A stepwise decrease in the heat capacity is observed. For the organic resins studied, it is shown that the glass transition temperature of the curing resin reaches the cure temperature at half of the decrease in heat capacity. Vitrification, the isothermal transition from a rubbery or liquid state to a glassy state, and the corresponding vitrification time can thus be measured in a single experiment.

A mobility factor is proposed which is based directly on the observed heat capacity evolution. This mobility factor is compared to the diffusion factor which is calculated from the modelled rate of reaction and the decrease in the rate of reaction at vitrification.

For the amine-cured and the anhydride-cured epoxies studied, both factors coincide and thus the mobility factor can be proposed as a direct measurement of the diffusion factor.

In contrast, the rate of reaction of the low-temperature formation of an inorganic polymer glass (IPG) is (nearly) uninfluenced by the vitrification process. The conversion increases long after vitrification and a glass transition temperature largely above the cure temperature can be reached. In this case, the diffusion and mobility factors do not coincide.

MDSC is shown to be a promising technique to study in more detail the effect of polymer microstructure and reaction mechanism on the interrelation between vitrification and the decrease in the rate of reaction due to mobility restrictions.

*Keywords:* Diffusion control; Heat capacity; Modulated differential scanning calorimetry; Thermosetting polymer; Vitrification

* Corresponding author.


*SSDI* 0040-6031(95)02693-2

## 1. Introduction

The network formation in thermosetting polymers has been studied extensively in the past. Thermal analysis techniques, and especially differential scanning calorimetry (DSC), have often been used to study reaction kinetics and the evolution of the glass transition temperature. Modulated differential scanning calorimetry™ (MDSC) is a recently developed extension of the conventional DSC technique which offers a new approach to material characterisation by thermal analysis [1–5].

In this work, the benefits of MDSC in studying the cure of thermosets and the vitrification process are evaluated. An epoxy–amine resin, an epoxy–anhydride resin, and a low-temperature inorganic polymer glass (IPG) were chosen to illustrate the abilities of MDSC. The IPG is an amorphous aluminosilicate formed by the low-temperature reaction of an alkaline sodium silicate solution (Sil) and a dehydroxylated clay (metakaolinite Mk) [6,7]. The behaviour of this inorganic network differs markedly from that generally observed for organic networks [7]. In this paper, attention is focused on the isothermal cure and vitrification; in a second contribution, non-isothermal cure will be considered [8].

A mobility factor obtained from the heat capacity evolution will be proposed and compared to the diffusion factor determined using the observed heat flow rate and a kinetic expression for the chemical rate. Differences in behaviour of the three systems will be discussed.

### 1.1. Modulated differential scanning calorimetry

The technique and extraction of the signals is introduced below. A more complete description can be found in the literature, e.g. in Refs. [1–3].

In MDSC a sample is subjected to a modulated temperature programme obtained by superimposing a sine wave on the conventional isothermal or linearly changing temperature programme

$$T = T_0 + \frac{\beta}{60} \cdot t + A_T \cdot \sin(\omega t) \tag{1}$$

where $T$ is the temperature in K, $T_0$ is the initial temperature in K, $\beta$ is the (linear) heating rate in K min$^{-1}$, $A_T$ is the temperature modulation amplitude in K, $\omega$ is the modulation angular frequency ($2\pi F$) in s$^{-1}$, and $t$ is the time in s.

This modulated temperature input gives rise to a modulated heat flow response which consists of an underlying and a cyclic heat flow signal. Assuming that the temperature modulation is small so that over the temperature interval of one modulation the response of the rate of the kinetic processes to the temperature can be approximated as linear, the heat flow response can be written as [1,3]

$$\frac{dQ}{dt} = C_p \cdot \left( \frac{\beta}{60} + A_T \cdot \omega \cdot \cos(\omega t) \right) + f(t, T) + A_K \cdot \sin(\omega t) \tag{2}$$

where $Q$ in J is the amount of heat transferred to the sample, $f(t, T)$ in W is the average response of a kinetic phenomenon to the underlying temperature programme, and $A_K$ in W is the amplitude of the kinetic response to the temperature modulation.

The underlying signals for both temperature and heat flow are calculated by an averaging process that subtracts the effects of the perturbation. The resulting underlying or total heat flow, $\phi_{tot}$ in W, and the underlying temperature reconstitute quantitatively the thermoanalytical curve measured by conventional DSC. Using a discrete Fourier transform algorithm, the cyclic component of both temperature input and heat flow response is extracted. Comparison of the amplitude of the cyclic heat flow, $A_{HF}$, with the amplitude of the heating rate, $A_T \cdot \omega$, results in an additional signal: the 'cyclic' heat capacity $C_p$ in $JK^{-1}$

$$C_p = \left( \frac{A_{HF}}{A_T \cdot \omega} \right) \tag{3}$$

Multiplying the heat capacity by minus the (measured) underlying heating rate gives the 'reversing' heat flow, $\phi_R$ in W; the non-reversing heat flow, $\phi_{NR}$ in W, is the difference between the total heat flow and the reversing heat flow (Eq. (4))

$$\begin{aligned} \phi_R &= -C_p \beta \\ \phi_{NR} &= \phi_{tot} - \phi_R \end{aligned} \tag{4}$$

Note that the extraction of the signals is done by a continuous integration, averaging and smoothing over more than one modulation period. For quantitative MDSC measurements, it is necessary to calibrate temperature and heat flow as in a conventional DSC; the heat capacity signal is calibrated using a reference material with a known heat capacity. For isothermal experiments, the reversing heat flow equals zero because of a zero underlying heating rate and, consequently, the non-reversing heat flow equals the total heat flow.

MDSC offers several advantages over conventional DSC. Events are separated into phenomena considered as reversible (R) and non-reversible (NR) material behaviour within the time scale of the perturbation, thus enabling a disentanglement of a number of overlapping thermal events, e.g. glass transition (R) and enthalpy relaxation (NR), and detection of metastable behaviour [1]. Using MDSC, the heat capacity and its evolution with time and temperature can be measured accurately for non-isothermal as well as for isothermal underlying temperature programmes. Other benefits are an improved resolution and an increased sensitivity for changes in heat capacity [1–5].

Over the recent years a number of articles have been published describing this technique [1,3–5] and the mathematical description of DSC measurements based on temperature modulation [2]. The experimental results published mainly discuss transitions in non-reactive polymer systems, such as the glass transition, cold crystallisation and melting of poly(hydroxybutyrate) [9], the glass transition and enthalpy relaxation in PET [10] and PET/PC blends [11] and the melting of PET [12]. In a recent publication, the influence of the modulation frequency and amplitude on the glass transition was studied for polystyrene [13]. For reactive systems, single experiments for an isothermal cure of an epoxy resin were reported [3–5] and results for the

isothermal low-temperature formation of an inorganic polymer glass (IPG) were briefly discussed [7].

### 1.2. Cure, vitrification, and rate of conversion

Curing thermosetting materials generally involves the transformation of low molecular weight liquids to amorphous networks with infinite molecular weight by means of exothermic chemical reactions. The chemo-rheological changes occurring can be rationalised using the isothermal temperature–time–transformation cure diagram [14–16]. The state of the material is governed by chemical conversion and temperature. Knowledge of the rate of cure and its dependence on temperature and conversion is important for predicting the course of the reaction for a certain thermal treatment.

When a thermosetting polymer is cured at a temperature substantially below the glass transition temperature of the fully cured network, $T_{g\infty}$, the glass transition temperature of the growing network, $T_g$ will rise to the cure temperature, $T_{cure}$. The attendant transition of a liquid state or rubbery state to a glassy state is called vitrification [14–16]. The chemical kinetics in the region near vitrification is often complicated by diffusion and/or mobility control [15,17]. In principle, the reaction can proceed until $T_g$ exceeds the cure temperature to that point where all chain movement ceases, so that the conformational entropy of the chain approaches zero, and the reaction stops due to the complete absence of mobility ($T_g$ approximately 50°C above $T_{iso}$, depending on the reacting system) [17]. This leads to a final conversion lower than unity in diffusion-controlled conditions. Note that the ultimate conversion can also be lower due to topological limitations, namely the fact that remaining reactive groups cannot meet and react even in the absence of any diffusion hindrance [18]. In any case, reaching this ultimate conversion would take an infinite time.

On transition to the glassy state, the rate of reaction drops sharply due to the onset of mobility control [15,17]. So, for accurately predicting the course of the reaction during the final stages of cure, it is necessary to correct the kinetic rate equation by a factor describing the effects of the decrease in mobility on the reaction rate. The rate equation covering the evolution of the reaction rate up to the final cure stages can be written as

$$\left(\frac{dx}{dt}\right)_{obs} = \left(\frac{dx}{dt}(x, T)\right)_{kin} \cdot DF(x, T) \tag{5}$$

where $x$ is the conversion and $(dx/dt)_{obs}$ the experimentally observed rate of conversion; $(dx/dt)_{kin}$ is the fictive rate of conversion in kinetically (or chemically) controlled conditions for the same conversion and temperature; this will be called the chemical rate. For autocatalytic reactions the chemical rate of reaction in the absence of mobility limitations can be described by an empirical rate equation

$$\frac{dx}{dt} = (k_1 + k_2 x^m)(1 - x)^n \tag{6}$$

with $k_1$ and $k_2$ rate constants and $m$ and $n$ reaction orders [19].

$DF$ is the diffusion factor correcting the chemical rate in conditions where mobility is constrained. This diffusion factor, governed by the viscoelastic state or the viscosity

of the material, ranges from 1 in the undisturbed state (no mobility constraints) to 0 in the frozen glass. The variation in the diffusion factor with conversion and temperature can be expressed as a function of the difference between the glass transition temperature $T_g$ and the cure temperature $T$ [15].

For amine-cured epoxies, Stutz and coworkers [17,20] used an approach based on the Vogel equation [21] resulting in a rate equation in the form of Eq. (5). To establish the evolution of the diffusion factor, Stutz first determined the rate expression for chemical control using conversion–time data in the initial cure states for temperatures largely above the initial glass temperature $T_{g0}$. The diffusion factor is obtained by taking the ratio of the observed rate of reaction over the chemical rate predicted. The results obtained for amine-cured epoxies lead to the conclusion that the structural units must undergo only small-angle rotational oscillations to allow for reaction [17,20]. This is in accordance with the observation that the cure reaction still proceeds in the glassy state where the segmental mobility, which provides for a translational diffusion of the functional groups in the rubbery or liquid system, is frozen out [18].

### *1.3. Heat capacity, vitrification, and mobility*

Vitrification of a thermosetting system was studied in the past using the different techniques. In torsional braid analysis (TBA) [14,16], the transition to the glassy state can be observed by a peak in the loss (shear) modulus and by a strong rise in the elastic (shear) modulus. The same approach can be used for dynamic mechanical analysis (DMA) when using a special set-up [7]. In dielectric thermal analysis (DETA), a peak in the loss factor and a decrease in permittivity are observed when vitrification takes place [22]. These techniques, however, give no quantitative information about the evolution of the conversion or rate of conversion with cure.

In DSC, vitrification can also be observed indirectly as a decrease in the rate of reaction when the material vitrifies. By doing multiple isothermal experiments for various reaction times, and measuring $T_g$ and conversion of the partially reacted sample in a subsequent non-isothermal residual cure, it is possible to determine whether a complex evolution of a reaction exotherm is due to kinetic or mobility (vitrification) effects [15]. However, this technique gives no direct information about the diffusion factor. To establish this factor, a model for the kinetically controlled reaction is needed.

Because heat flow and heat capacity are measured simultaneously, MDSC offers a great opportunity for studying the rate of conversion and vitrification behaviour of a thermosetting system. Cassettari and coworkers [23,24] have used a differential microcalorimeter especially designed to enable the simultaneous measurement of heat capacity and the rate of enthalpy release. The $C_p$ measurement employed is based on the measurement of the relaxation of the temperature difference between sample and reference cell after a power pulse. Thus, in this technique the heat flow rate is perturbed with a known heat flow pulse and the variation of the sample temperature is measured, whereas in modulated DSC the sample temperature is perturbed sinusoidally and the resulting heat flow is measured. The differential microcalorimeter employed by Cassettari allows only for isothermal measurements; with MDSC, non-isothermal experiments can also be performed [8].

During an isothermal cure, the motions of the polymer chain segments are increasingly hindered due to the growing crosslink density of the network; this limits the number of available conformational and vibrational states [25]. This reduction in chain segment mobility causes a decrease in heat capacity $C_p$ of the material: the contribution of conformational mobility to $C_p$ in the rubbery or liquid state is strongly reduced upon vitrification. This decrease in $C_p$, provoked by the isothermal transition of a rubbery or liquid state to a glassy state by network formation, is comparable to the decrease in heat capacity observed when cooling a non-reactive material to a temperature below its $T_g$.

It is clear that the restriction of the segmental mobility and the change in heat capacity upon vitrification are closely linked: starting from an initial $C_{pl}$ in conditions where no mobility restrictions exist, there is an isothermal change to a final $C_{pg}$ for a state in which all chain movement has ceased. In the light of this relation between segmental mobility and heat capacity, in this work a new mobility factor $DF^*$ is proposed which is based on the evolution of $C_p$ in an isothermal experiment (7)

$$DF^*(t, T) = \frac{C_p(t, T) - C_{pg}(T)}{C_{pl}(t, T) - C_{pg}(T)} \tag{7}$$

This mobility factor $DF^*$, changing from unity for initial conditions to zero for the final glassy state, can be determined experimentally by measuring the evolution of $C_p$ for an isothermal cure at a specified temperature $T$. Note that $C_{pl}$ changes with curing time, as will be pointed out below. The mobility factor is obtained directly from the experiment, in contrast to the approach of the previous paragraph where a model for the chemical kinetics is needed to calculate the diffusion factor.

## 2. Experimental

### 2.1. Raw materials and processing

*2.1.1. Epoxy resins* The amine-cured epoxy consisted of a tetra-functional epoxy (Araldite MY 720) and a stoichiometric amount of tetra-functional amine hardener (HY 2954), with an epoxy equivalent weight (EEW) and amine equivalent weight of 125 g $eq^{-1}$ and 59.5 g $eq^{-1}$ respectively.

The anhydride-cured epoxy consisted of a bifunctional DGEBA-type epoxy (LY 556, EEW = 183–192 g $eq^{-1}$, $n = 0.13$), a tetra-functional anhydride hardener (methyltetrahydrophthalic anhydride HY 917, anhydride equivalent weight = 166 g $eq^{-1}$), and an accelerator (1-methyl imidazole DY 070). The components were mixed in a LY 556/HY 917/DY 070 weight ratio of 100/90/1, resulting in a stoichiometric epoxy–anhydride mixture.

The chemical structure of the reactants is given in Fig. 1. All components are from Ciba-Geigy and were used without purification. The prescribed amounts of the components were added to a weighed amount of epoxy. A magnetic stirrer was employed at room temperature to obtain a homogeneous mixture. The recipient was sealed hermetically and stored at −20°C.

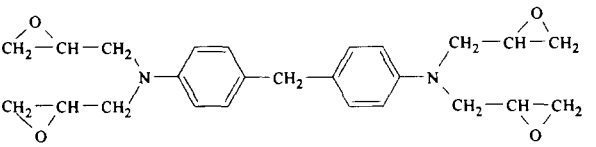

N,N,N',N'-tetraglycidyl-4,4'-diaminodiphenylmethane (MY 720)

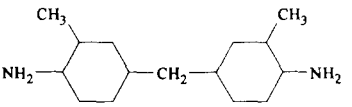

3,3'-dimethyl-4,4'-diaminodicyclohexylmethane (HY 2954)

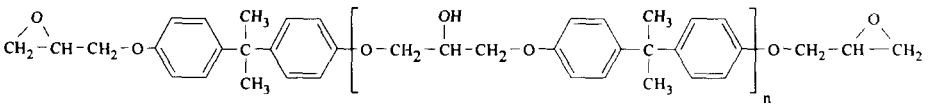

diglycidyl ether of bisphenol A (LY 556)

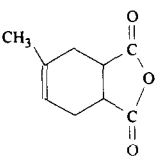

methyltetrahydrophtalic anhydride (HY 917)

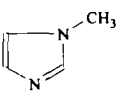

1-methyl imidazole (DY 070)

Fig. 1. Chemical structure of the organic reactants.

*2.1.2. The inorganic polymer glass* The inorganic polymer glass (IPG) consisted of an amorphous aluminosilicate formed by the low-temperature reaction of an alkaline sodium silicate solution (Sil) with a dehydroxylated clay (metakaolinite Mk), defined as $(Na_2O)(SiO_2)_{1.4}(H_2O)_X$ ($X$ represents the bound water in the solution) and $(Al_2O_3)(SiO_2)_2(H_2O)_{0.05}$ respectively. For the sodium silicate solution (Sil), molar

ratios of $SiO_2/Na_2O = 1.4$ and $H_2O/Na_2O = 10$ were used. The molar ratio Sil/Mk used was 1. The overall reaction can be written as:

$$(Na_2O)(SiO_2)_{1.4}(H_2O)_X \quad (Sil) + (Al_2O_3)(SiO_2)_2(H_2O)_{0.05} \quad (Mk) \xrightarrow{\text{aq.}(\leq 100\,^\circ C)} (Na_2O)(Al_2O_3)(SiO_2)_{3.4}(H_2O)_Z \quad (IPG) \tag{8}$$

where $Z$ is about 0.4 [6]. The materials and the sample preparation were described previously [6].

### 2.2. *Analytical techniques: instrumentation, calibration and experimental procedure*

The MDSC measurements were performed in a TA *Instruments* 2920 DSC with MDSC™ option and equipped with a refrigerated cooling system. Helium was used as the purge gas (25 ml $min^{-1}$). Temperature was calibrated using cyclohexane and indium. Indium was used for the enthalpy calibration. The heat capacity was calibrated with a linear polyethylene reference material NIST SRM 1475 [26] at 150°C ($C_p = 2.57$ $J\,g^{-1}\,K^{-1}$ [27]) for the organic systems and with a 50/50 mixture by weight of kaolinite KGa – 1 ($C_p = 0.956$ $J\,g^{-1}\,K^{-1}$ [28]) and water ($C_p = 4.180$ $J\,g^{-1}\,K^{-1}$ [29]) at 25°C for the IPG. For the calibrations, the same pan type, sample heat capacity (sample weight times specific heat capacity), and period were used as in the corresponding experiments. The experimental error on the heat capacity values cited was about 2%.

·Hermetic aluminium pans (TA *Instruments*) were used for the organic systems. The sample weight used was 10–20 mg. Quasi-isothermal experiments with a modulation amplitude of 0.5°C and a 60 s period (0.5°C per 60 s) were performed. For partial cure reactions, the isothermal experiment was halted at a predetermined time and the residual reaction enthalpy, $\Delta H_{res}$, and the glass transition temperature, $T_g$, were measured by first cooling the partially reacted sample to −50°C and then heating to 275°C at 2.5°C $min^{-1}$ with a 0.3°C per 60 s modulation.

The total reaction enthalpy, $\Delta H_{tot}$, measured in a conventional DSC experiment at 10°C $min^{-1}$ amounts to −530 and −335 J $g^{-1}$ for the epoxy–amine and anhydride systems respectively.

For the IPG system, reusable high-pressure stainless steel sample pans (Perkin–Elmer) were used, withstanding an internal pressure of 150 atm. The pan weights were about 630 mg and were matched on sample and reference sides. It was necessary to use these high pressure pans because free water is present during the reaction and the temperature is increased up to 300°C in non-isothermal experiments (as for residual cure). For quasi-isothermal experiments, the sample was scanned at 20°C $min^{-1}$ to its isothermal temperature where a modulation of 0.5°C and 100 s was superimposed. The total reaction enthalpy measured for a heating at 5°C $min^{-1}$ without modulation equals −230 J $g^{-1}$ [6].

A 0.5°C amplitude was chosen for the quasi-isothermal experiments to achieve a sufficient sensitivity for the heat capacity measurement. For non-isothermal experiments, the amplitude chosen results in an only-heating condition. For the IPG

experiments, the period was increased to 100 s because of the higher thermal mass of the high pressure pans.

The influence of the modulation frequency on the experimental results was not studied in this work. However, the range of frequencies that can be used in practice is limited, so that no strong effects are expected.

### 2.3. Calculation

The time at half of the heat capacity change, $t_{0.5\Delta Cp}$, was calculated as the time at half-height of the difference between the extrapolated tangents. The heat capacity change, $\Delta C_p$ is the difference between the extrapolated tangents evaluated at $t_{0.5\Delta Cp}$.

For isothermal experiments the conversion $x$ at a reaction time $t$ is the ratio of the partial reaction enthalpy evolved since the start of the experiment $\Delta H_p(t)$, and the total reaction enthalpy $\Delta H_{tot}$. The rate of conversion was obtained by dividing the non-reversing heat flow by the total reaction enthalpy.

For partially reacted samples, conversion and glass transition temperature were determined in a subsequent heating. The conversion is determined as

$$x = 1 - \frac{\Delta H_{res}}{\Delta H_{tot}} \tag{9}$$

with $\Delta H_{res}$ the residual reaction enthalpy. The glass transition temperature $T_g$ was calculated as the temperature at half height of the heat capacity change. This implies that it was evaluated for the modulation period imposed (60 s).

## 3. Results and discussion

### 3.1. Amine- and anhydride-cured epoxy resins

The epoxy–amine resin was cured quasi-isothermally at a temperature ($T_{iso}$) of 70°C. Fig. 2 shows the non-reversing heat flow and heat capacity as a function of reaction time. The non-reversing heat flow agrees well with the heat flow evolution for a conventional DSC experiment performed under the same conditions with the exception of the modulation (not shown). This is also an indication of the fact that the temperature modulation is not influencing the reaction kinetics. The reaction exotherm obeys an autocatalytic behaviour: the heat flow increases at first and passes through a maximum. The heat capacity $C_p$ first increases slightly; subsequently a stepwise decrease in $C_p$ is observed, simultaneously with a sharp decrease in heat flow. A $C_p$ value of 1.84 J $g^{-1}$ $K^{-1}$ is attained at the end of the reaction exotherm. The heat capacity change equals 0.62 J $g^{-1}$ $K^{-1}$. The time at half the heat capacity change, $t_{0.5\Delta Cp}$, equals 97 min.

The evolution of both the reaction conversion, $x$, and glass transition temperature, $T_g$, with reaction time for this quasi-isothermal cure at 70°C was determined from a residual cure of a number of partially reacted samples (Fig. 3). The initial $T_g$ for uncured epoxy–amine amounts to −23°C. $T_g$ surpasses the reaction temperature $T_{iso}$

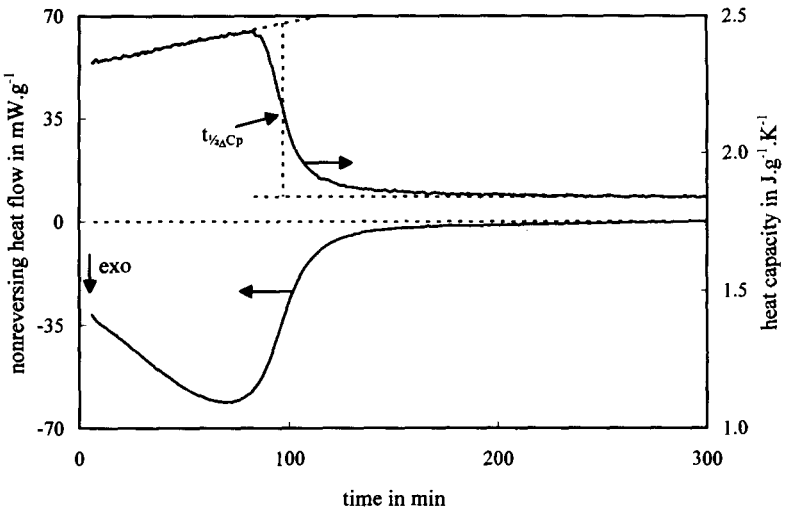


Fig. 2. Non-reversing heat flow and heat capacity $C_p$ for the quasi-isothermal cure of an epoxy–amine at 70°C with a 0.5°C per 60 s modulation; $t_{0.5\Delta Cp}$ is the time at half of the decrease in heat capacity.

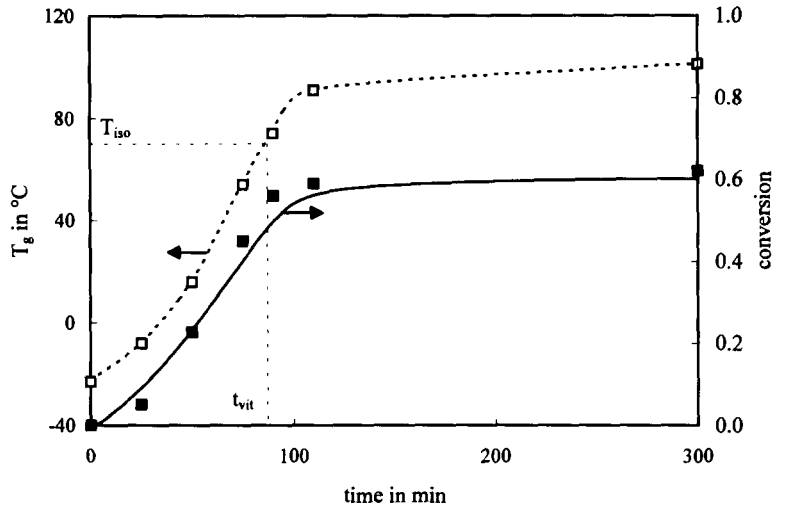


Fig. 3. Evolution of the conversion, $x$, and the glass transition temperature, $T_g$, for the quasi-isothermal cure of an epoxy–amine at 70°C with a 0.5°C per 60 s modulation: conversion (■) and $T_g$ (□) measured in a subsequent heating, and conversion obtained by numerical integration of the isothermal reaction exotherm (———); $t_{vit}$ is the time when $T_g$ equals $T_{iso}$.

after 88 min ($t_{vit}$) and levels off to reach a $T_g$ of 103°C for 60% conversion after 300 min. Comparison of the evolution of $C_p$ and $T_g$ (Figs. 2 and 3) shows that the time $t_{0.5\Delta Cp}$ corresponds very well to the time $t_{vit}$. Therefore, $t_{0.5\Delta Cp}$ obtained in a modulated DSC experiment can be used to quantify the time of vitrification. This time can be interpreted

as the time at which half of the material has transformed to the glassy state (on the time scale of the modulation).

Before the onset of vitrification (at a conversion of 40%), the heat capacity increases linearly with conversion. For the cure of a DGEBA epoxy resin with ethylenediamine, an increase in $C_p$ with reaction time has also been mentioned by Cassettari et al. [23,25]. This change in $C_p$ due to reaction is taken into account when calculating the mobility factor (Eq. (7)) because the latter should only include the reduction of the segmental mobility contribution to $C_p$ due to vitrification, and not variations due to changes caused by the reaction itself. The observed variation in $C_p$ was incorporated into Eq. (7) by changing the heat capacity $C_{pl}$ linearly with conversion using an extrapolation of the data before vitrification. The mobility factor $DF^*$ can then be calculated from the observed heat capacity evolution.

To derive the diffusion factor from the heat flow data, a rate expression is needed for describing the rate of conversion $dx/dt$ in chemically controlled conditions. For reaction times below the onset of vitrification, the autocatalytic rate Eq. (6) is fitted to the experimental rate of conversion versus time profiles. The resulting rate constants and reaction orders can be used to calculate the evolution of conversion and rate of reaction in the absence of mobility restrictions. Fig. 4 compares the conversion in the isothermal experiment at 70°C with the conversion obtained by numerical integration of the chemical rate equation. Up to the onset of vitrification, both curves coincide. When vitrification takes place, the experimental rate of conversion (the slope of the conversion curve) quickly decreases; a limiting conversion $x_{lim}$ is reached for high reaction times. In the absence of mobility restricting effects, conversion keeps increasing and will finally reach unity.

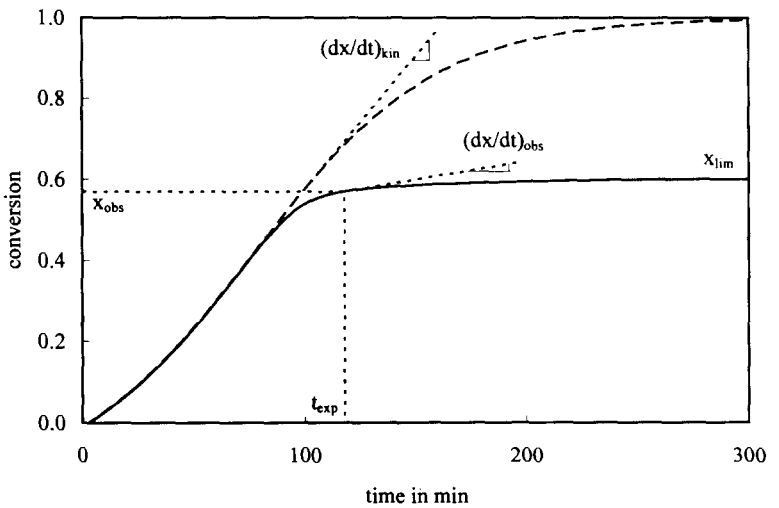


Fig. 4. Conversion versus reaction time for the cure of an epoxy–amine at 70°C. Experimental profile (——) and profile calculated for chemical control (------); $x_{lim}$ is the ultimate conversion reached isothermally.

For each reaction time $t_{exp}$, the experimental rate of conversion can be compared to the predicted chemical rate by comparing the slopes of the two curves for the same conversion $x_{obs}$. The resulting rate of conversion profiles are shown in Fig. 5. For each reaction time $t_{exp}$, the experimental rate $(dx/dt)_{obs}$ is plotted as well as the chemical rate $(dx/dt)_{kin}$ that would result for the experimental conversion $x_{obs}$ if there were no mobility limitations. Note that the chemical rate plotted does not correspond to the derivative of the conversion profile shown in Fig. 4 but to the rate calculated using Eq. (6) for the conversion $x_{obs}$. While the experimental rate decreases to zero for high reaction times, the chemical rate stays near its maximum. The ultimate experimental conversion is 60% and, as a consequence, a high concentration of unreacted functional groups is still present. So, if there were no mobility limitations for that specific conversion, the rate of conversion would be high, as reflected in Fig. 5.

The ratio of these rates results in the diffusion factor $DF$ (Eq. (5)). The evolution with reaction time of the heat flow diffusion factor $DF$ and the heat capacity mobility factor $DF^*$ is shown in Fig. 6. Both factors, originating from two different experimental quantities, give quantitatively the same evolution and almost coincide.

A second organic thermosetting system, an anhydride-cured epoxy resin, was reacted isothermally at temperatures ranging from 60 to 120°C. For the quasi-isothermal cure at 85°C, the evolution of non-reversing heat flow and heat capacity is shown in Fig. 7. The reaction is again autocatalytic: a maximum heat flow is reached after 52 min. The final isothermal conversion is 86%, attained for a reaction time of 400 min; $T_g$ measured in the subsequent heating equals 105°C. The time at

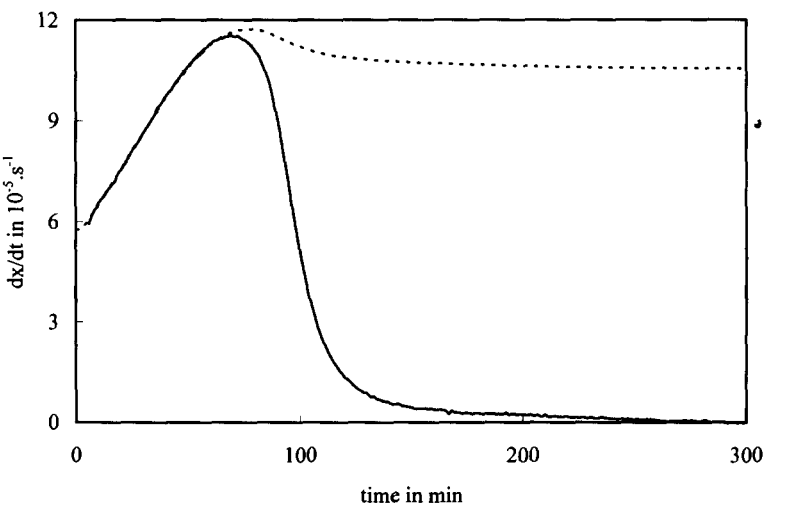


Fig. 5. Rate of conversion versus reaction time for the cure of an epoxy–amine at 70°C. Experimental rate $(dx/dt)_{obs}$ (——) and rate expected for the conversion $x_{obs}$ in the absence of mobility restrictions, $(dx/dt)_{kin}$ (------).

half of the change in $C_p$ equals 200 min and corresponds to a conversion of 82%. No sharp drop in heat flow is observed in this region but the reaction rate is already low. $C_p$ is virtually constant up to the onset of vitrification; $\Delta C_p$ at $t_{0.5\Delta Cp}$ equals $0.37\,J\,g^{-1}\,K^{-1}$.

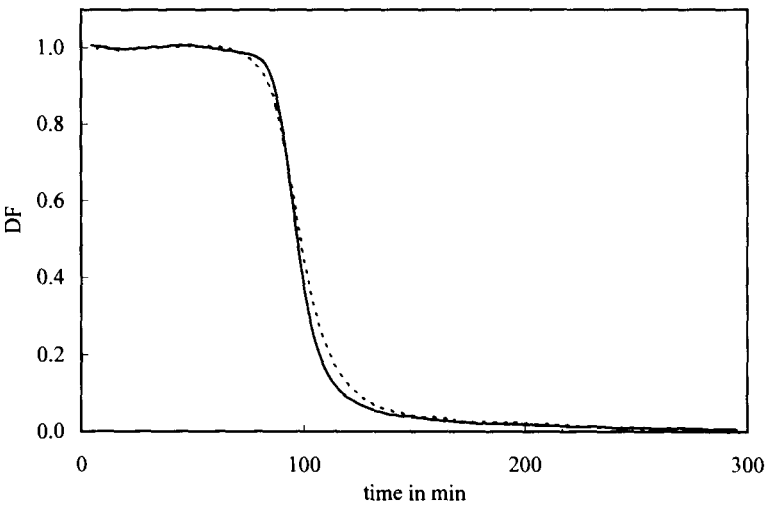


Fig. 6. The cure of an epoxy–amine at 70°C: comparison of the mobility factor based on heat capacity (——) and the diffusion factor based on heat flow (------).

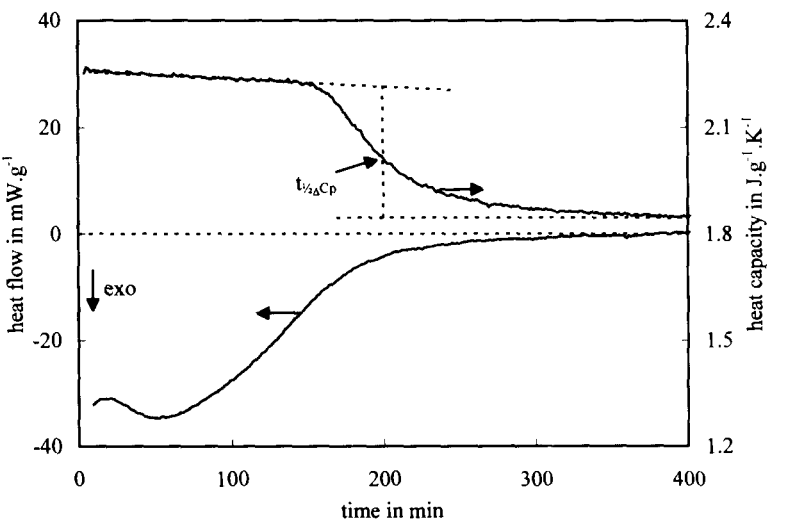


Fig. 7. Non-reversing heat flow and heat capacity $C_p$ for the quasi-isothermal cure of an epoxy–anhydride at 85°C with a 0.5°C per 60 s modulation.

Another experiment at 85°C was stopped at a reaction time of 200 min ($t_{0.5\Delta Cp}$). The glass transition temperature in the residual heating is 83°C: this implies that $t_{0.5\Delta Cp}$ corresponds to the time $t_{vit}$ that $T_g$ equals the reaction temperature, as for the amine-cured epoxy.

Before vitrification starts, a small heat capacity decrease is observed (Fig. 7) as opposed to a heat capacity increase for the epoxy–amine. This decrease is seen for all reaction temperatures and is linear with conversion up to conversions as high as 80% (at 120°C). The slope of the decline increases for the highest reaction temperature. The change in $C_p$ with reaction is again taken into account for calculating the mobility factor.

Fig. 8 shows the evolution of the factors *DF* and *DF**, obtained in the same way as for the amine-cured epoxy: the two curves again nearly coincide. The mobility factor *DF** for the epoxy–anhydride reaction at different reaction temperatures is shown in Fig. 9. All curves show a stepwise decrease in *DF** at vitrification; with increasing temperatures, the change occurs at lower reaction times.

### 3.2. *The low-temperature formation of an inorganic polymer glass*

The low-temperature formation of an amorphous aluminosilicate (IPG) was studied quasi-isothermally at 35°C for 800 min. The reaction exotherm shows a typical behaviour with the maximum reaction rate at the start of the experiment followed by a shoulder of more or less constant rate (Fig. 10). The heat capacity remains nearly

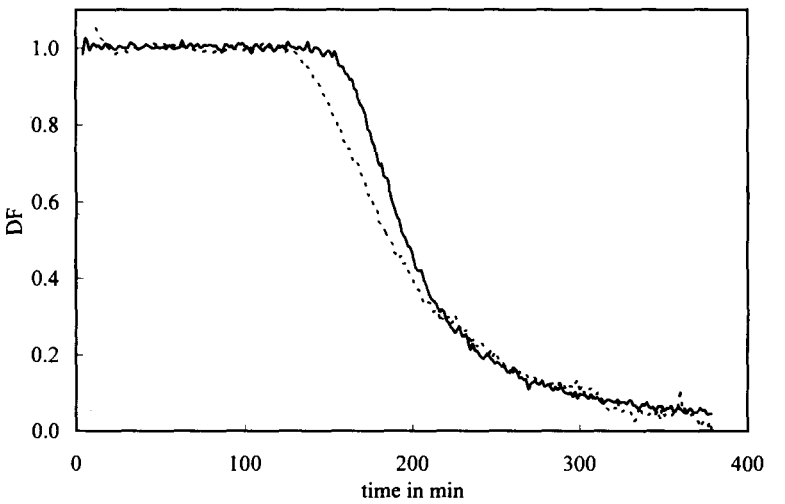


Fig. 8. The cure of an epoxy–anhydride at 85°C: comparison of the mobility factor based on heat capacity (——) and the diffusion factor based on heat flow (------).

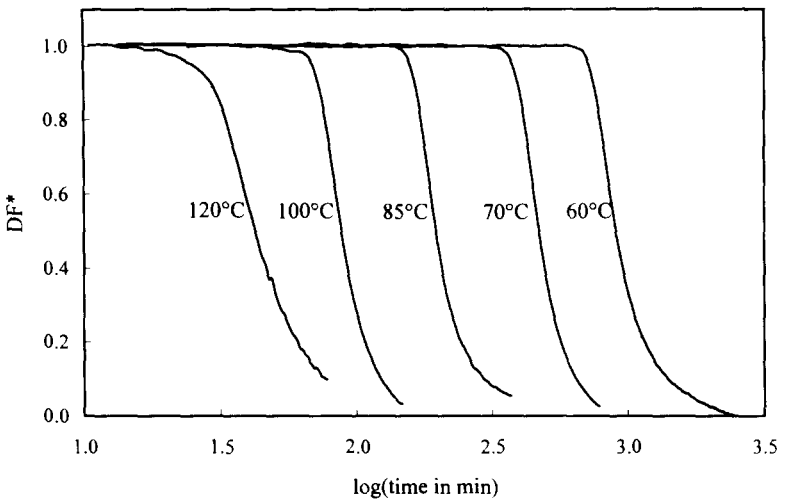


Fig. 9. Evolution of the mobility factor *DF** with time for the quasi-isothermal reaction of an anhydride-cured epoxy at temperatures ranging from 60 to 120°C (logarithmic time scale).

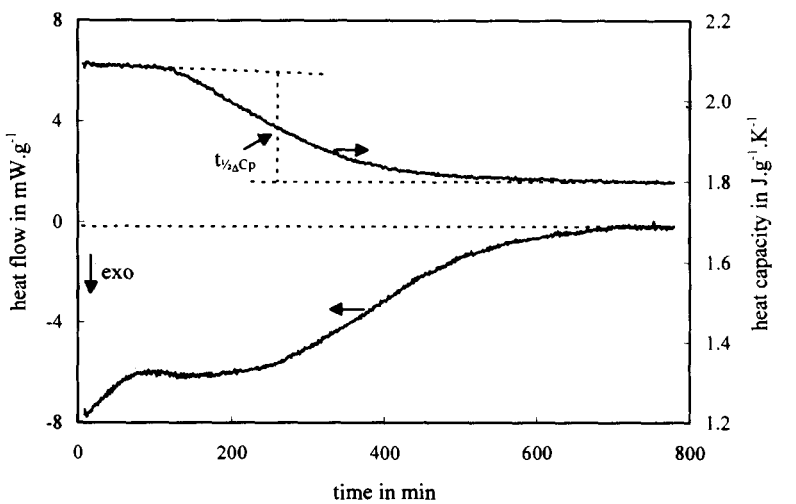


Fig. 10. Non-reversing heat flow and heat capacity $C_p$ for the quasi-isothermal cure of an inorganic polymer glass (IPG) at 35°C with a 0.5°C per 100 s modulation.

constant up to 20% conversion, then a gradual decrease is observed resulting in a $\Delta C_p$ equal to 0.27 J g$^{-1}$ K$^{-1}$ at $t_{0.5\Delta Cp}$ equal to 245 min. The rate of reaction stays more or less the same over the first half of the change in $C_p$ and decreases slowly over the second half. At the end of the reaction exotherm, a conversion of 75% is reached (based on a total reaction enthalpy of $-230$ J g$^{-1}$). A residual heating shows a peak ($-57$ J g$^{-1}$) setting in at about 175°C and with a maximum at 238°C. In the second heating, no glass transition is observed before the onset of the residual reaction exotherm (where $T_g$ starts increasing again), leading to the conclusion that $T_g$ has risen to at least 175°C during the isothermal cure at 35°C [8].

Earlier work on the cure of an IPG showed that the onset of the decrease in $C_p$ measured with MDSC corresponds to the onset of vitrification defined by the strong rise in elastic modulus measured with dynamic mechanical analysis (DMA) [7]. This indicates again that $t_{0.5\Delta Cp}$ can be used as a measure for the vitrification time.

The diffusion factor *DF* and mobility factor *DF** were calculated using the same procedures as for the organic resins. This time the diffusion factor *DF* stays near unity long after the decrease in the mobility factor *DF** (Fig. 11): $C_p$ nearly reaches its final value before *DF* starts decreasing too.

### 3.3. Comparison of the thermosetting systems

Table 1 summarises the results obtained for the three thermosetting systems. For the epoxy–anhydride reaction at 60°C, the conversion and the rate of conversion cannot be assessed quantitatively. The experiment had a duration of 2500 min and the maximum heat flow is around 100 μW for a 10 mg sample. Using the TA *instruments* refrigerated cooling system, the baseline stability over these long experiments is better than 20 μW,

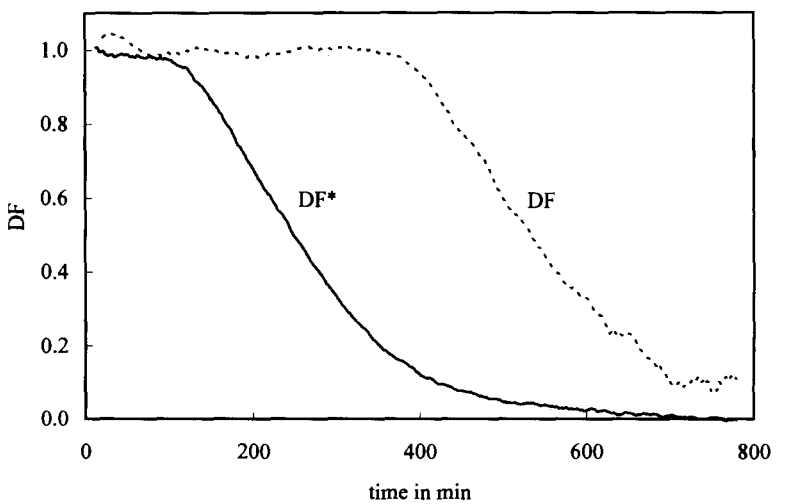


Fig. 11. The reaction of an inorganic polymer glass (IPG) at 35°C: comparison of the mobility factor based on heat capacity (———) and the diffusion factor based on heat flow (------).

Table 1
Results for the isothermal vitrification of three thermosetting systems at the reaction temperature $T_{iso}$. $t_{0.5\Delta C_p}$ is the time at half decrease of $C_p$ (vitrification), $x_{vit}$ and $(dx/dt)_{vit}$ are conversion and rate of conversion at vitrification; $\langle dx/dt \rangle$ is the mean rate of conversion before vitrification ($= x_{vit}/t_{vit}$) and $r$ is the ratio of $(dx/dt)_{vit}$ over $\langle dx/dt \rangle$; $x_{iso}$ and $T_{giso}$ are the conversion and glass transition temperature reached at the end of the isothermal experiment as measured in a subsequent heating

| | $T_{iso}$/°C | $t_{0.5\Delta C_p}$/min | $x_{vit}$ | $(dx/dt)_{vit}/10^{-5}s^{-1}$ | $\langle dx/dt \rangle/10^{-5}s^{-1}$ | $r$ | $x_{iso}$ | $T_{giso}$/°C |
|---|---|---|---|---|---|---|---|---|
| Epoxy–amine | 70 | 97 | 0.53 | 6.3 | 9.1 | 1:1.4 | 0.60 | 103 |
| Epoxy–anhydride | 60 | 920 | [a] | [a] | [a] | [a] | 0.78 | 81 |
| | 70 | 470 | 0.76 | 0.6 | 2.7 | 1:4.5 | 0.80 | 85 |
| | 85 | 200 | 0.82 | 1.4 | 7.0 | 1:5 | 0.86 | 105 |
| | 100 | 89 | 0.89 | 1.5 | 17 | 1:11 | 0.90 | 111 |
| | 120 | 50 | 0.97 | 0.6 | 32 | 1:53 | 0.97 | 128 |
| IPG | 35 | 245 | 0.45 | 2.8 | 3 | 1:1.1 | 0.75 | > 175 |

[a] These values could not be assessed quantitatively (see text).

which for the 60°C measurement nevertheless amounts to a 20% error on the heat flow. Therefore, the baseline needed to derive heat flow and conversion could not be quantitatively determined for this experiment. Additional improvement of the experimental conditions can probably further reduce this baseline drift. The changes in heat capacity can, however, be measured accurately because this measurement depends only on the response to the modulation. In other words, even for very slow reactions vitrification can be followed quantitatively in a single MDSC experiment, but to determine accurately the evolution of the conversion for reactions with a maximum heat flow of less than 100 μW, the conventional approach of multiple partial reactions followed by a residual heating should be used.

Comparison of the results for the three thermosetting systems shows clearly different relations between vitrification and the rate of reaction.

First consider the organic resins: the conversion $x_{vit}$ attained at vitrification of the epoxy–anhydride is more than 20% higher than for the amine-cured epoxy. This is related to a different evolution of $T_g$ with conversion (Fig. 12). For the amine-cured epoxy, both resin and hardener are tetra-functional, whereas a bifunctional epoxy is used with the anhydride. Therefore, $T_{g\infty}$ for the amine-cured epoxy is higher due to a higher final crosslink density and, while curing this system, the increasing glass transition temperature will reach the isothermal reaction temperature $T_{iso}$ at a lower conversion than for the anhydride system.

The higher conversion $x_{vit}$ for the anhydride system causes the onset of mobility limitations to be seen near the end of the reaction exotherm (Fig. 7), whereas for the amine system, vitrification sets in near the maximum reaction rate (Figs. 2 and 5). To evaluate the results more quantitatively, the rate of conversion at vitrification $(dx/dt)_{vit}$ can be compared to the average rate before vitrification, $\langle dx/dt \rangle$, which equals $x_{vit}/t_{vit}$. It is necessary to work with ratios or relative rates $r$ (Table 1) because the amine-cured epoxy is much more reactive than the anhydride system. This is reflected in a vitrifica-

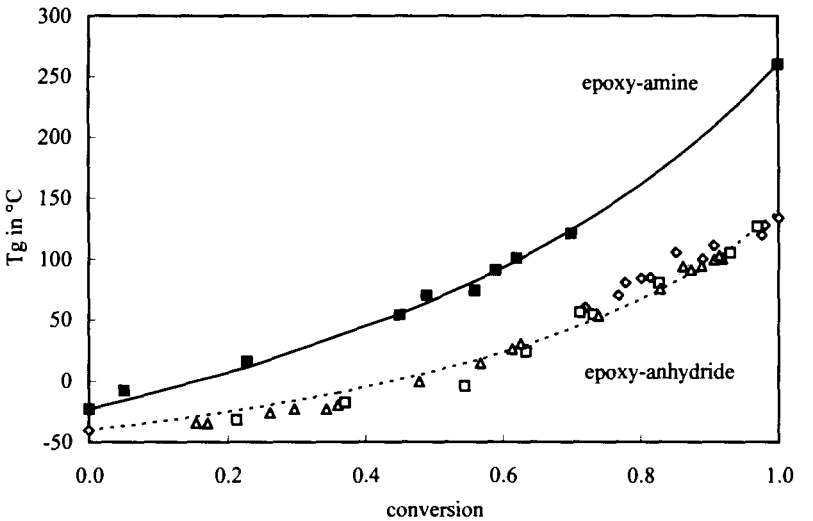


Fig. 12. Glass transition temperature $T_g$ as a function of conversion for the amine-cured and anhydride-cured epoxy resins. Experimental points ($T_g$, $x$) were measured in a heating subsequent to an isothermal cure experiment. Curves were obtained by fitting a model for the $T_g$–$x$ relation [14].

tion time that is five times lower for the epoxy–amine compared to the epoxy–anhydride at the same temperature. For the anhydride-cured epoxy, the ratio $r$ of $(dx/dt)_{vit}$ to $\langle dx/dt \rangle$ is lower than 1:4, which is much smaller than a ratio of 1:1.4 for the amine-cured epoxy. The ratio $r$ also decreases with increasing cure temperature (for the epoxy–anhydride).

Variations of this ratio correlate with the differences in the final isothermal cure state. Since the rate of conversion at vitrification is non-zero, conversion further increases in the (partially) glassy state (although more slowly, Fig. 4). Therefore $T_g$ increases to values above the reaction temperature $T_{iso}$. For the epoxy–anhydride, this difference $T_{giso} - T_{iso}$ decreases from 21 to 8°C with increasing reaction temperature; for the epoxy–amine the difference is 33°C. The changes observed are in the same trend as the evolution of the relative rate at vitrification; a relatively lower $(dx/dt)_{vit}$ or ratio $r$ corresponds to a smaller increase in conversion between vitrification, $x_{vit}$, and the end of the reaction exotherm, $x_{iso}$, and thus to a smaller increase in $T_g$ beyond $T_{iso}$. The increase in $T_g$ evidently also depends on the slope of the $T_g$–$x$ curve for $x_{vit}$. For both the epoxy–amine and the epoxy–anhydride, the slope at $x_{vit}$ amounts to about 4°C per % of conversion. This agrees well with the increase in $T_g$ after vitrification except for the epoxy–anhydride at 100 and 120°C where the experimental error on the small increase in conversion after vitrification more strongly affects the ratio $\Delta T_g/\Delta x$.

These results seem to indicate that the epoxy–amine reaction is less hindered by the occurrence of vitrification than the epoxy–anhydride reaction is: for the former system, conversion, and as a consequence $T_g$, increase more in the glassy state. This can be corroborated from a more chemical point of view.

For a step polymerisation reaction to take place, the two reacting entities have to move toward each other by translational diffusion and segmental diffusion and

rotation. Besides other parameters, the mobility needed for reaction is determined by the distances separating the functional groups.

At vitrification the concentration of reactive units in the epoxy–amine is approximately 4 times higher compared to the epoxy–anhydride, due to a higher initial concentration and a lower conversion at vitrification. Postulating an equal distribution of non-reacted units, at vitrification the mean distance to the nearest reaction partner, termed the reaction distance, is 8 Å for the epoxy–amine and 13 Å for the epoxy–anhydride. In the glass transition region, a mobility of about 30–50 chain segments is available, depending on the specific chemical structure [30], allowing for reaction while the material is vitrifying. The reaction can continue in the glassy state, reaching a $T_g$ higher than $T_{iso}$, until the increasing crosslink density restricts the mobility of shorter chain segments (or until reaction distances become larger than mobility allows for). Due to the smaller reaction distances, the epoxy–amine requires less mobility to react, and, since crosslink density is coupled to $T_g$, a relatively higher $T_g$ can be reached before the mobility is so strongly restricted that the reaction is halted.

Due to the structures of the tetra-functional epoxy and amine (Fig. 1), the partially reacted network is prone to cyclisation [31,32]. Such short-distance intramolecular cyclisation reactions can probably still take place when the material is vitrifying. The formation of the small cycles will decrease the number of chain ends and increase the stiffness of the macromolecules, thus contributing to a further increase in conversion and $T_g$. No cyclisation is observed for the DGEBA-type epoxies used in the epoxy–anhydride [31,32]. These points again correlate well with the higher increase in conversion and $T_g$ of the amine-cured epoxy in the glassy state.

For the organic resins, the mobility and diffusion factors coincide. This means that the mobility needed for reaction and the mobility frozen out at vitrification are of a comparable molecular scale. Because the factors are equivalent, the heat-capacity-based mobility factor, derived directly from the MDSC experiment, can be used to predict the decrease in the rate of reaction upon vitrification. This also allows for plotting lines of constant mobility factor (and diffusion factor) on the TTT diagram with the line for $DF^*$ equal to 0.5 corresponding to the vitrification line.

As a second step, the results for the organic thermosetting polymers can be compared to those for the inorganic polymer glass. The differences evolve more or less in the same sense as when changing from an anhydride-cured to an amine-cured epoxy (Table 1). Vitrification, defined as the decrease in heat capacity, occurs at low conversion, while the reaction rate is still near its maximum, but, as opposed to observations for the organic resins, no marked decrease in the rate of reaction is observed at that time. The conversion increases another 30% before the end of the reaction exotherm; a glass transition temperature of more than 175°C is reached for an isothermal cure at 35°C. For the IPG, no $T_g - x$ evolution is available because it is impossible to determine $T_g$ for intermediate conversions: on heating a partially reacted sample, the residual reaction exotherm starts before the glass transition is seen [8]. However, this fact is intrinsically in accordance with a reaction continuing in the vitrified state. After polymerisation and elimination of free water, $T_g$ is around 650°C [7].

On a molecular scale, the glass transition in inorganic polymer networks differs quite markedly from the transition in polymers: it is a chemical process, corresponding to an

equilibrium of bond breaking and formation, enabling reorganisations to take place [7,33,34]. The reaction of metakaolinite and sodium silicate solution to a network of $SiO_4$ and $AlO_4$ tetrahedra in which no Al–O–Al bonds occur [6], is probably a short-range reorganisation, not involving the movement (translational diffusion) of large entities. Small molecules and ions ($H_2O$, $OH^-$, $Na^+$) are known to play an important role in the reaction mechanism [6,7]. The results indicate that the reaction is not impeded upon vitrification of the material, therefore the transition from a liquid to a glass is not a physical barrier for the low-temperature cure of IPG. The reaction continues until mobility on a smaller molecular scale is restricted.

The evolution of the diffusion factors (Fig. 11) agrees well with this previous discussion. The decrease in diffusion factor *DF* happens long after the decrease in mobility factor *DF** (vitrification).

However, for the IPG, caution is needed when interpreting this heat flow diffusion factor *DF*. Its evolution depends strongly on the model used for describing the chemical reaction rate. In this work, the autocatalytic rate equation was used to fit the rate of conversion profile. Since the onset of effects of mobility restrictions on the reaction rate is not known, the curve was fitted as far in conversion as possible, taking care not to lose fit quality for the lower conversions. The diffusion factor obtained should thus be considered as a first approximation. For a less empirical determination, a more mechanistic approach has to be used for proposing a reaction model, which is not straightforward due to the heterogeneous nature of the reaction.

In any case, the fact that the diffusion and mobility factors do not coincide for the IPG indicates that care has to be taken when using the experimentally determined mobility factor to predict the cure rate of a material in conditions of mobility control. When the molecular motions frozen out at vitrification do not correspond to the molecular motions needed for reaction, the mobility and the diffusion factor will be shifted in time: if mobility limitations on the rate of reaction only become important when mobility is restricted on a smaller molecular scale than the motions constrained at vitrification, the heat flow diffusion factor *DF* will be shifted toward higher conversions as compared to the mobility factor *DF**.

## 4. Conclusions

This work has focused on the study of the possible benefits in using modulated DSC to study the isothermal cure of thermosets.

The observed stepwise decrease in the heat capacity during an isothermal cure experiment can be identified with the vitrification of the network formed. When the organic resins vitrify, the reactions slow down due to mobility restrictions. For the organic systems studied, the mobility factor based on heat capacity proposed in this work almost coincides with the diffusion factor defined as the ratio of the observed rate of reaction over the rate predicted by chemical kinetics modelling (in the absence of diffusion control). The information needed is contained in a single quasi-isothermal MDSC experiment by the generation of the cyclic heat capacity curve.

The formation of an inorganic polymer glass is (nearly) uninfluenced by vitrification: the rate of reaction only decreases at the end of the vitrification process, and a glass

transition temperature largely above the cure temperature is reached. This is attributed to short-distance reactions requiring less mobility than the mobility that is frozen out at vitrification; the mobility needed for reaction is only frozen out long after vitrification occurred.

These results indicate that MDSC is a very promising technique for studying thermosetting systems in general. Temperature–time–transformation (TTT) diagrams, which can be employed for improving the processing conditions for curing thermosetting resins, could be developed further. The evolution of the heat capacity mobility factor at different reaction temperatures permits the construction of lines of equal mobility restrictions, including the vitrification line, on the time–temperature–transformation diagram. Using the heat capacity mobility factor proposed, the effects of polymer structure and reaction mechanism on the deceleration of the reaction could be studied and theoretical models for the diffusion factor could be evaluated.

## Acknowledgements

The authors would like to thank L.C. Thomas of TA Instruments for many fruitful discussions. The work of G. Van Assche and A. Van Hemelrijck was supported by grants from the Flemish Institute for the Promotion of Scientific-Technological Research in Industry (I.W.T.).

## References

[1] M. Reading, A. Luget and R. Wilson, Thermochim. Acta, 238 (1994) 295.
[2] B. Wunderlich, Y. Jin and A. Boller, Thermochim. Acta, 238 (1994) 277.
[3] M. Reading, Trends Polym. Sci., 1 (1993) 248.
[4] P.S. Gill, S.R. Sauerbrunn and M. Reading, J. Therm. Anal., 40 (1993) 931.
[5] M. Reading, D. Elliot and V.L. Hill, J. Therm. Anal., 40 (1993) 949.
[6] H. Rahier, B Van Mele, M. Biesemans, J. Wastiels and X. Wu, J. Mater. Sci., submitted for publication, part A.
[7] H. Rahier, B Van Mele, M. Biesemans, J. Wastiels and X. Wu, J. Mater. Sci., submitted for publication, part B.
[8] G. Van Assche, A. Van Hemelrijck, H. Rahier and B. Van Mele, Thermochim. Acta, in press.
[9] A. Cesaro, L. Navarini and R. Pepi, Thermochim. Acta, 227 (1993) 157.
[10] S.R. Sauerbrunn, R.L. Blaine and J.A. Foreman, Proc. 22nd NATAS Conf., Denver, USA, Sept. 19–22, 1993, p. 514.
[11] S.R. Sauerbrunn, P.S. Gill and C.J. Marcozzi, Proc. 22nd NATAS Conf., Denver, USA, Sept. 19–22, 1993, p. 313.
[12] S.R. Sauerbrunn and L.C. Thomas, Proc. 23rd NATAS Conf., Toronto, Canada, Sept. 25–28, 1994.
[13] A. Boller, C. Schick and B. Wunderlich, Proc. 23rd NATAS Conf., Toronto, Canada, Sept. 25–28, 1994, p. 26.
[14] J.K. Gillham and J.B. Enns, Trends Polym. Sci., 2 (1994) 406.
[15] G. Wisanrakkit and J.K. Gillham, J. Coat. Technol., 62 (1990) 35.
[16] M.T. Aronhime and J.K. Gillham, Adv. Polym. Sci., 78 (1986) 83.
[17] H. Stutz, J. Mertes and K. Nuebecker, J. Polym. Sci. Part A: Polym. Chem., 31 (1993) 1879.
[18] B.A. Rosenberg, Adv. Polym. Sci., 75 (1986) 75.
[19] M.R. Kamal, Polym. Eng. Sci., 14 (1974) 231.

[20] H. Stutz and J. Mertes, J. Polym. Sci. Part A: Polym. Chem., 31 (1993) 2031.
[21] H. Vogel, Phys. Z., 22 (1921) 645.
[22] S.D. Senturia and N.F. Sheppard, Jr., Adv. Polym. Sci., 80 (1986) 1.
[23] M. Cassettari, G. Salvetti, E. Tombari, S. Veronesi and G.P. Johari, J. Polym. Sci. Part B: Polym. Phys., 31 (1993) 199.
[24] M. Cassettari, F. Papucci, G. Salvetti, E. Tombari, S. Veronesi and G.P. Johari, Rev. Sci. Instrum., 64 (1993) 1076.
[25] M. Cassettari, G. Salvetti, E. Tombari, S. Veronesi and G.P. Johari, J. Non-Cryst. Solids, 172–174 (1994) 554.
[26] National Institute of Standards and Technology, Standard Reference Materials Program, SRM 1475—Linear Polyethylene, Gaithersburg, 1993.
[27] V.B.F. Mathot and M.F.J. Pijpers, J. Therm. Anal., 28 (1983) 349.
[28] R.A. Robie and B.S. Hemingway, Clays and Clay Minerals, 39 (1991) 362.
[29] Osborne, Stimson and Gennings, in R.C. Weast (Ed.), CRC Handbook of Chemistry and Physics, CRC Press, Boca Raton, Florida, 70th edn., 1989, p. D-173.
[30] L.H. Sperling, Introduction to Physical Polymer Science, Wiley-Interscience, New York, 2nd edn., 1992, p. 311.
[31] L. Matějka and K. Dušek, Macromolecules, 22 (1989) 2902.
[32] L. Matějka and K. Dušek, Macromolecules, 22 (1989) 2911.
[33] J.M. Jewell, C.M. Shaw and J.E. Shelby, J. Non-Cryst. Solids, 152 (1993) 32.
[34] O.V. Mazurin, J. Non-Cryst. Solids, 129 (1991) 259.